Optical Fiber Delay-Line Signal Processing

KENNETH P. JACKSON, MEMBER, IEEE, STEVEN A. NEWTON, MEMBER, IEEE, BEHZAD MOSLEHI, MEMBER, IEEE, MOSHE TUR, C. CHAPIN CUTLER, LIFE FELLOW, IEEE, JOSEPH W. GOODMAN, FELLOW, IEEE, AND H. J. SHAW, FELLOW, IEEE

Abstract—**Single-mode optical fiber is an attractive delay medium for processing microwave frequency signals due to its extremely low loss (< 0.1 dB/μs) and large available time–bandwidth product (in excess of 10^5). Recent progress in the efficient tapping of light from single-mode fibers has made it possible to construct recirculating and nonrecirculating (tapped) delay-line structures that can perform a variety of important signal processing functions. These functions include coded sequence generation, convolution, correlation, matrix–vector multiplication, and frequency filtering. This paper presents the fundamental properties of single-mode fiber delay lines and reviews recent experimental results that demonstrate the feasibility of fiber delay-line devices for broad-band signal-processing applications.**

I. Introduction

THE USE OF OPTICAL FIBER is revolutionizing many areas of science and engineering. A relatively new kind of fiber that guides an optical signal in a single transverse power distribution, or mode, is proving to be particularly useful in the areas of communications [1] and environmental sensing [2]. Single-mode optical fiber is capable of accurately transmitting modulated signals with bandwidths exceeding 100 GHz over a 1-km distance [3] with losses less than 0.5 dB [4]. Since only one mode is guided, its phase and polarization (a superposition of two polarization modes) can be determined at any point along the length of the fiber. As a result, single-mode fibers can be used as flexible optical paths in interferometers that sense environmental effects which perturb the fiber and thus the relative phase of the guided light.

While single-mode optical fiber has been used most often in connection with communication and sensing systems, it can also be used in configurations that are capable of processing broad-band signals. Signal-processing operations are possible because of the excellent propagation and delay properties. The low loss and low dispersion of single-mode fiber allows signals to propagate large distances without significant attenuation or distortion.

The propagation and delay properties of single-mode fiber are particularly attractive because digital signal-processing and conventional analog signal-processing techniques (such as those using surface acoustic-wave devices) are limited in their usefulness for signal bandwidths exceeding one or two gigahertz, although they are very effective at lower frequencies. However, for applications requiring very high data rates, bandwidths of 10 GHz and beyond may be needed. Therefore, devices that can process signals having bandwidths of many gigahertz can be of importance for a wide variety of applications. The real-time processing of broad-band radar signals is an example of a current application that would benefit from devices of this kind. Potential applications include the direct interfacing of fiber processors with high-speed optical communications systems. Likewise, fiber systems can perform real-time processing operations on the optical output of one or more fiber sensors, including the time-division multiplexing of slow sensor outputs to match the high data rates that can be handled by fiber systems. In either case, the ability to process broad-band optical data before transduction into electrical signals can be of great practical value.

In the work reviewed here, the approach has been to use single-mode fiber and single-mode fiber components to build recirculating and nonrecirculating delay lines. Recirculating and nonrecirculating delay-line filters have been used as the basic format for a wide variety of devices that have used many different delay media. For example, delay-line filters can be built by simply connecting lengths of coaxial cable. More sophisticated approaches use metal-on-silicon (MOS) processing techniques to fabricate charge-coupled devices (CCD's) [5] capable of providing long delays (up to 1 s) and typically operating at frequencies of about 10 MHz and below.

Acoustic-wave delay-line devices are perhaps the most widely used approach for signal-processing applications [6]–[8]. The most versatile and sophisticated of the acoustic delay-line devices are those that use surface acoustic waves (SAW's) [9]. Planar processing techniques can be used to fabricate SAW transversal filters that have thousands of taps and can operate at frequencies as high as several hundred megahertz.

New technologies are emerging that may provide delay-line filters operating at frequencies well above 1 GHz. Magnetostatic-wave (MSW) devices, which make use of the propagation of slow, dispersive spin waves in low-loss ferromagnetic materials [10], can operate at center frequencies in the range of 2–12 GHz with bandwidths on the order of 1 GHz. Superconducting delay-line (SDL) filters [11], [12], using niobium transmission lines and proximity coupler taps, promise to offer low-loss devices with bandwidths as large as 20 GHz.

The use of optical fiber as a delay medium for signal-processing applications was proposed by Wilner and van den Heuvel [13], who noted that fiber delay lines were

Manuscript received March 5, 1984; revised September 27, 1984. This work was supported in part by Litton Systems, Inc.

K. P. Jackson, B. Moslehi, C. C. Cutler, J. W. Goodman, and H. J. Shaw are with Stanford University, Stanford, CA 94305.

S. A. Newton is with Hewlett-Packard Laboratories, Palo Alto, CA 94304.

M. Tur is with the School of Engineering, Tel Aviv University, Tel Aviv, Israel.

0018-9480/85/0300-0193$01.00 ©1985 IEEE

attractive due to their low loss and low dispersion. Ohlhaber and Wilner [14] reported an experimental demonstration of an optical fiber transversal filter. This experiment used three multimode fiber delay paths to generate and correlate a 4-bit, 88-Mb/s coded sequence. An optical fiber frequency filter was demonstrated by Chang, Cassaboom, and Taylor [15], who illuminated a bundle of fifteen multimode fibers that provided fifteen different delays spaced by 5.2 ns. The outputs from these fibers were incident on a single detector yielding a filter with a transfer function having a fundamental passband at 193 MHz. Many specific applications of optical fiber delay-line filters have since been proposed by Taylor [16] and others. The most recent experimental demonstration (aside from those described in this paper) was that of Rausch, Efurd, and Corbin [17], who used two multimode fiber delay lines to generate and correlate a 2-bit, 1-Gb/s Barker code.

These previous demonstrations of optical fiber delay-line filters have used individual multimode fiber delay paths from source to detector. These devices are therefore subject to the bandwidth limitations of multimode fiber (~1 GHz-km) and, in some implementations, are limited to a small number of taps due to the practical difficulties of uniformly illuminating and detecting light from a large number of bundled fibers. Thus, if the full potential of optical fiber delay lines is to be realized, it is necessary to make devices featuring many taps on a solitary single-mode fiber delay line. In this way, the extremely large bandwidth and low loss of single-mode fiber can be exploited.

The difficulties involved in constructing a single-mode fiber delay-line filter are that of making efficient and reproducible taps on a single-mode fiber. The objectives of the work presented in this paper have been to investigate possible tapping mechanisms, to develop fabrication techniques to implement these mechanisms, and to demonstrate the performance of basic signal-processing functions through the development of single-mode fiber delay-line filter prototypes. The development of these prototypes in turn provided a foundation for the implementation of single-mode fiber delay-line networks capable of synthesizing many sophisticated time- and frequency-domain filtering operations. This paper reviews the fundamental delay-line properties of single-mode fiber, the basic features of optical fiber signal-processing devices, and the fabrication and experimental demonstration of three different single-mode fiber delay-line filters. In addition, the implementation of single-mode fiber delay-line networks, incorporating recirculating and nonrecirculating delay lines, is discussed including theoretical formulations for analyzing these networks and experimental demonstrations of simple processing functions.

II. Optical Fiber Delay Lines

The merits of a delay medium for a particular delay-line application can be determined by examining several important parameters. For broad-band signal processing, these parameters include loss, dispersion, and linearity. In this section, these and other important characteristics are discussed as they relate to optical fiber in general, and single-mode fiber in particular.

A. Loss

Attenuation in optical fibers results from a number of wavelength-dependent mechanisms including scattering [18], absorption [19], and externally induced losses, such as those due to bending [20]. Each of these losses can be small over a particular range of optical wavelengths. However, the combined effect of these losses restricts the operation of fiber systems to a relatively narrow spectral band from the visible to the near infrared (0.6–1.6 μm).

Rayleigh scattering is the dominant loss mechanism in optical fibers below a wavelength of about 1.6 μm. This loss mechanism is due to the scattering of the propagating electromagnetic wave by small (on the order of a few tenths of a micron) irregularities in the medium. The attenuation coefficient per unit length for Rayleigh scattering is proportional to λ^{-4}. As a result, the attenuation is much lower at longer wavelengths than at shorter wavelengths. For example, the loss per unit length at $\lambda = 0.83$ μm is on the order of 3 dB/km, whereas the loss per unit length at $\lambda = 1.3$ μm is on the order of 0.5 dB/km (1 km corresponds to 5 μs of delay).

At longer wavelengths, infrared absorption losses, resulting from the vibration of the bonds between the glass constituents, limit most optical fiber systems to operation at wavelengths of about 1.6 μm and below. These absorptive losses combined with Rayleigh scattering loss yield a composite loss profile with a minimum (~ 0.2 dB/km) near 1.5 μm. For the devices described in this paper, sources having wavelengths of 0.82 μm were used. At this wavelength, the intrinsic propagation loss is dominated by Rayleigh scattering and is approximately 3 dB/km.

An important characteristic that sets optical fiber apart from other delay media is that at a given source wavelength the propagation loss of the fiber is independent of the modulating signal frequency. This characteristic is illustrated in Fig. 1 in which the propagation loss is plotted as a function of signal frequency at the wavelength of minimum loss. For comparison, the propagation loss for other delay-line media are included. As indicated in Fig. 1, the propagation loss of optical fiber is significantly lower at high signal frequencies than that of other media for a comparable delay time.

B. Dispersion (Bandwidth Limitations)

Several different kinds of dispersion can contribute to limit the bandwidth of optical fiber. The dominant dispersive mechanism depends on the waveguide properties of the fiber and the spectrum of the optical source.

The modulation bandwidth of multimode fiber is most severely limited by modal dispersion. Multimode fiber can guide a number of transverse modes that do not, in general, travel at the same group velocity. As a result, the fidelity with which high-frequency components of an analog signal may be transmitted is limited. Modulation bandwidths of multimode fiber are typically in the range of a

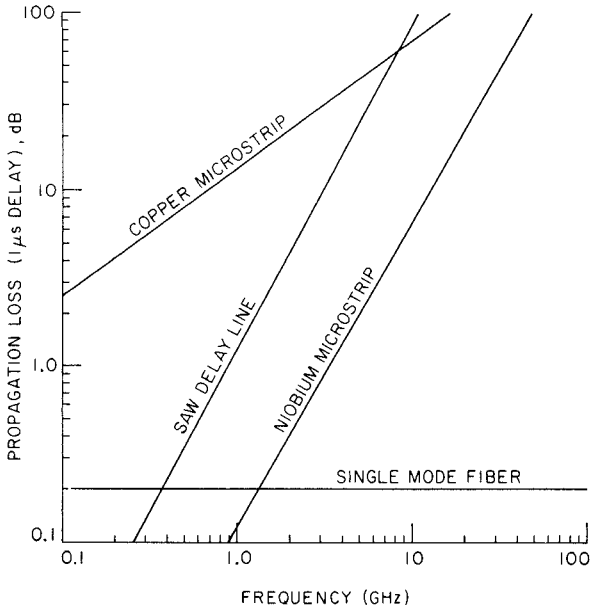

Fig. 1. Propagation loss per 1 μs of delay as a function of signal frequency for single-mode fiber and other delay-line media. Propagation losses for nonfiber delay media have been calculated using typical values.

few MHz-km to several hundred MHz-km. Bandwidths of just over 1 GHz-km can be obtained using multimode fiber with a graded index profile. Such an index profile is designed to minimize modal dispersion by equalizing the optical paths of the various modes.

While this bandwidth in fact is sufficient for most of the delay-line devices discussed in this paper, single-mode fiber is required for devices that provide long delays. Since all of the power coupled into a single-mode fiber propagates in a single transverse mode, modal dispersion is absent. As a result, high-frequency signals can potentially be transmitted accurately over longer distances than are possible with multimode fiber.

The modulation bandwidth of single-mode fiber is typically limited by the dependence of the fiber refractive index on the wavelength of the optical carrier (material dispersion). This limitation is due to the different group delays suffered by different spectral components of the source. It can be shown for carrier wavelengths of 1.06 μm and below, the 3-dB optical bandwidth is given approximately by [21]

$$f_{3\text{dB}} \approx \frac{187.3}{\sigma L \left| \frac{d\tau_g}{d\lambda} \right|} \tag{1}$$

where $f_{3\text{dB}}$ is the modulation bandwidth of the fiber in gigahertz, L is its length, $|d\tau_g/d\lambda|$ (ps/nm-km) is the differential dispersion with τ_g equal to the group delay per unit length, and σ is the rms half-width of the spectrum of the optical source. The width of the source spectrum includes the presence of modulation sidebands. As an example, a laser diode source having a spectral width of $\sigma =$ 2 nm at a wavelength of $\lambda = 820$ nm produces a differential dispersion of approximately -100 ps/nm-km. The single-mode fiber bandwidth–distance product at this wavelength is therefore approximately 0.94 GHz-km. Although most of the delay-line devices reported have utilized sources with wavelengths at 0.82 μm, the length of fiber in these devices was much less than a kilometer. As a result, material dispersion did not significantly limit the bandwidth of these devices even though the wavelength of the source was not optimal.

In general, however, it is desirable to operate at a wavelength where the differential dispersion tends to zero. At this wavelength (≈ 1.3 μm), the bandwidth of the fiber can become quite large ($\gtrsim 100$ GHz-km); it is limited primarily by higher order dispersion effects and by polarization dispersion, which is due to the difference in group delay between the two polarization modes supported by the fiber.

These potentially large modulation bandwidths coupled with the relatively long delays that are possible with single-mode fiber can provide large time–bandwidth products. Assuming a bandwidth–distance product of 100 GHz-km and a delay per unit length of 5 μs/km, the achievable time–bandwidth product exceeds 10^5.

C. Linearity (Dynamic Range)

The fundamental (i.e., exclusive of the limitations imposed by a source or detector) linear dynamic range of optical fiber is limited by quantum noise at one extreme and by nonlinear loss processes at the other. The minimum detectable power transmitted by a low-loss fiber is limited by quantum noise, defined by the noise equivalent power (NEP) [22]:

$$\text{NEP} = 2h\nu B, \tag{2}$$

where h is Planck's constant, ν is the spectral frequency of the signal, and B is the bandwidth (inversely proportional to the measurement period).

The upper limit to the linear power-handling capabilities of the fiber is set by stimulated Raman and stimulated Brillouin scattering. The primary effect of these scattering processes is to transfer energy from the propagating input wave to either a forward or backward propagating wave at a lower frequency (longer wavelength). For many broadband signal-processing applications, the detection system is not strongly wavelength selective. As a result, the dynamic range of the fiber is limited only by stimulated Raman and stimulated Brillouin backscattering. Of these two backward processes, only stimulated Raman is significant. Stimulated Brillouin scattering can be neglected since in many cases the power within any frequency interval of about 50 MHz is less than a particular threshold value. This condition is satisfied even when single-frequency sources are used, because broad-band modulation will distribute much of the power into wide modulation sidebands.

The generation of stimulated Raman backscattering in low-loss optical fiber has been treated in detail [23]. The critical input power P_{crit} above which stimulated Raman backscattering becomes important is given roughly by

$$P_{\text{crit}} \approx 21 \frac{A}{\gamma_0 L} \tag{3}$$

where A is the cross-sectional area of the fiber core, L is the fiber length, and γ_0 is the Raman gain coefficient. Assuming $\gamma_0 = 5 \times 10^{-10}$ cm/W [24], and a 200-m (1-μs delay) length of single-mode fiber having a 6-μm-diam core, the critical power level is $P_{crit} \approx 0.6$ W. For a 2-m (10-ns delay) length of the same fiber, the critical power level is on the order of 60 W. The assumptions that went into obtaining (3) predict values for the critical input power that are lower than those obtained in practice. In addition, (3) assumes a CW input. For the pulsed case, the expression is modified by an effective interaction length to take into account the finite duration of the pulse.

Given (2) and (3), the inherent dynamic range of transmission in single-mode fiber can be estimated. While the Raman scattering is essentially independent of the signal (modulation) frequency, the quantum noise is linearly proportional to the signal bandwidth. Therefore, the fundamental optical dynamic range of a fiber delay line decreases linearly with increasing signal bandwidth. This dependence is shown graphically in Fig. 2, in which the dynamic range is plotted as a function of the signal bandwidth for two different delay lengths at a wavelength of $\lambda = 0.82$ μm. As is evident in the figure, the fundamental optical dynamic range for the transmission of a 10-GHz signal along a 200-m (1-μs) delay line exceeds 80 dB.

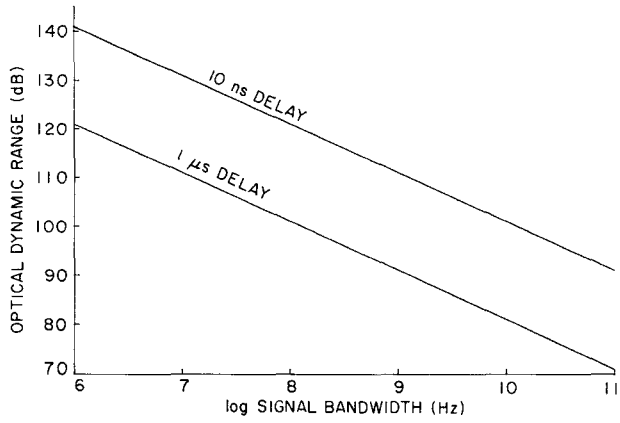

Fig. 2. Fundamental optical dynamic range of single-mode fiber as a function of modulation signal bandwidth.

D. Other Considerations

Optical fiber has several other favorable characteristics that are relevant to its use as a delay medium for signal processing. For example, optical fiber is relatively flexible, thereby allowing the construction of small, compact devices. Moreover, the flexibility of the fiber will not lead to any significant bending losses, provided the fiber is not bent below a critical radius. The critical bend radius is dependent on the wavelength and the waveguide properties of the fiber, and is typically several millimeters for commercially available fiber.

Another favorable characteristic of optical fiber delay lines is that the time intervals between taps can be made with great precision due to the high velocity of light in the medium. The group velocity of light in fiber is roughly 2×10^8 m/s. Thus, if the spacing between fiber taps is known to within 1 mm, the time delay between them is known to within 5 ps.

Fiber delay lines are also relatively insensitive to environmental effects when they are operated in an incoherent mode (to be discussed in the next section). Although the optical path provided by single-mode fiber may change by several optical wavelengths due to pressure and temperature fluctuations [2], fiber delay-line devices are only affected by gross effects that change the optical path length by an amount on the order of the modulation envelope of the signal. For example, a change in temperature of 140°C would cause a 0.1-percent variation in delay.

Finally, optical fiber is insensitive to electromagnetic interference. This characteristic is advantageous, not only for fiber signal-processing devices, but also for fiber sensors and transmission systems. Signal-processing devices are often used in electromagnetic environments that can interfere with the operation of conductive delay-line devices. The immunity of fiber to such interference, along with its light weight, makes optical fiber a desirable delay medium.

III. Signal Processing with Optical Fiber Delay Lines

In many ways, optical fiber delay-line devices are schematically similar to delay-line filters made using more conventional technologies, such as devices using surface acoustic waves. As a result, many of the signal-processing functions implemented with fiber delay lines are operationally similar to those implemented with conventional technologies. The basic design methods and processing structures developed for these conventional approaches can be applied to optical fiber implementations as well.

However, certain features exist that are special to optical fiber delay lines that must be considered when applying these design methods. These features relate to the fact that signals to be processed are represented by the modulation envelope of an optical carrier. As a consequence, some fiber-optic delay-line configurations have restrictions on the types of signals that can be processed.

In this section, these features and their effects on fiber delay-line signal processing are discussed. In addition, basic fiber-optic processing structures used to perform a variety of time-domain and frequency-domain operations are presented. The presentation of these structures focusses on the schematic representation; the exact fiber-optic implementation will be left for later sections in which specific delay-line devices are presented.

A. Incoherent Signal Processing

Optical fiber delay-line signal processing is set apart from other delay-line techniques by fundamental differences that stem from the fact that most optically encoded signals are modulated onto a carrier whose frequency is thousands of times greater than that of the highest signal frequency component. Optical detectors are square-law devices that respond to the incident optical power and none is fast enough to respond to the carrier frequency. This is in contrast to the situation encountered in a surface

acoustic-wave delay line, where interdigital electrodes with finger spacings corresponding to the spatial period of the acoustic carrier directly detect a propagating acoustic wave. The propagating acoustic wave induces a voltage on the electrodes proportional to the amplitude of the acoustic wave at that point.

This example illustrates a basic difference between optical fiber delay lines and conventional delay lines. Whereas conventional delay lines coherently combine tapped signals, optical fiber delay-line filters (in their present form) incoherently combine tapped signals resulting in the addition of optical powers.

In principle, the optical carrier can be utilized for coherent processing. In this case, the relative phases of the optical carrier of each tapped signal must be stable to within a fraction of an optical wavelength. This requires a narrow source spectrum that is highly stable as well as differences in optical paths that are constant to within a fraction of an optical wavelength. Such coherent systems can be difficult to implement in practice and are usually more complicated than incoherent systems because of the stringent requirements on the stability of the source and optical delay paths. For this reason, coherent detection, which depends on the phase of the optical carrier, is avoided in single-mode fiber delay lines.

To insure that coherent interference of the optical carrier is minimal, techniques providing spatial and temporal averaging of the carrier are employed. When tapped portions of a temporally coherent carrier impinge on a detector from different angles, a phase variation exists in the plane of the detector. Since this phase variation is quite large for small angular separations, the detector averages over the area of the wavefront intercepted by the detector. This yields an output proportional to the sum of the optical powers. Even if spatial averaging is not present, a carrier with a broad range of frequency components is used thus providing temporal averaging of the signal components. If tapped outputs of a delay line are spatially coherent, but the carrier has a broad spectrum, then the frequency components of the carrier will beat against each other and be effectively averaged over time provided the detector integration time is sufficiently long. The necessary condition for obtaining temporal averaging is given by

$$\tau_c \ll T_{\text{int}} \ll T_0 \tag{4}$$

where T_0 is the time delay between tapped signals, T_{int} is the integration time of the detector, and τ_c, the coherence time of the carrier, is given roughly by $\tau_c \sim 1/\Delta\nu$.

Fortunately, semiconductor laser diodes can exhibit both a broad output spectrum and the ability to be directly modulated at speeds up to several gigahertz. They are therefore the sources of choice for most optical fiber delay-line applications.

B. Positivity

One important consequence of incoherent summation in fiber delay-line filters is that negative weighting of taps cannot be accomplished optically. The power extracted from a fiber delay line can be weighted by attenuation (or amplification) before detection. However, since power is an inherently positive quantity, it cannot be optically manipulated to add to zero with other incident optical power if the effects of coherent interference are eliminated. For time-domain applications, encoding algorithms exist which allow bipolar, or in general, complex signal weightings [25]. For frequency-domain as well as time-domain applications, bipolar weightings can be implemented by collecting the tapped outputs with either of two separate detectors that are electrically inverted with respect to each other. For example, a code having both positive and negative values was cross-correlated by using a second inverting detector to distinguish the negative weighting [26].

The devices described in this paper utilize mostly positive weightings that are accomplished optically by attenuation. Devices of this kind fall into the category of *positive systems*. The application of positive systems theory to optical fiber delay-line devices is useful in that general conclusions about their behavior can be ascertained without knowing the details of their construction, operation, and the exact values of device parameters. For example, the magnitude of the transfer function of an optical fiber filter can nowhere exceed its value at the origin [27]. Also, information about the locations of the poles and zeroes of the transfer function of a fiber filter can be obtained. For instance, it can be shown that there cannot be an odd number of zeroes to the right hand of the pole with the largest magnitude (which is real and positive).

C. Fiber-Optic Structures and Applications

A generalized fiber-optic processing system that includes an optical source, an optical fiber delay-line device, and a square-law photodetector is shown in Fig. 3. Input electrical power $\mathscr{P}_{\text{in}}$ drives an optical source via an input voltage v_{in} or an input current i_{in} that is proportional to the square root of the electrical power. The source may be an external modulator whose applied voltage determines the amount of transmitted power from a CW optical source. More commonly, the optical source is a semiconductor laser diode whose output can be directly modulated by an input current. If the laser is operated in the linear portion of its diode characteristic (as indicated in Fig. 3), the optical power transmitted to the input of the fiber device P_{in} is linearly proportional to the input current.

The optical power output of the fiber delay line is linearly proportional to the input optical power, provided the optical input power does not induce nonlinear effects (as described in the previous section) and that coherent interference effects are not significant. The optical power output P_{out} is detected by a square-law detector with the detector photocurrent linearly proportional to the intensity striking its sensitive surface. The output current i_{out} is proportional to the square root of the electrical output power $\mathscr{P}_{\text{out}}$.

The entire system can be treated as a linear, time-invariant system in which the output is the convolution of the input with the impulse response of the device. Given

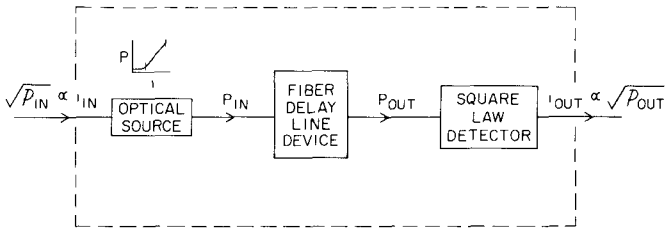

Fig. 3. Generalized fiber processing system that includes an optical source, fiber delay-line device, and photodetector.

these properties, the response of these devices can be analyzed using classical transform techniques.

It is important to point out that the evaluation of these fiber systems depends on whether electrical power or optical power has been specified. For some applications, the response of these fiber systems to electrical power is of importance, whereas in other applications, the response of the system to optical power may be important. Since the electrical power is proportional to the square of the optical power, improper evaluations can result from inaccurately specified parameters.

The fiber delay-line device depicted in Fig. 3 can be one of several configurations. Two configurations that are basic to fiber-optic signal processing are the recirculating delay line (Fig. 4(a)) and the nonrecirculating, or tapped delay line (Fig. 4(b)). The recirculating delay line consists of a loop of fiber which has been partially closed upon itself (shown schematically with a fiber directional coupler—see Section IV-B). Signals introduced into one end of the delay line recirculate around the loop producing outputs on each transit. The tapped delay-line structure consists of a fiber which has taps distributed along its length. Signals introduced into one end of the delay line are successively sampled, weighted, and then incoherently summed either by optical summation before detection or by electronic summation after detection.

The tapped delay line and the recirculating delay line can perform a variety of signal-processing functions. For example, both can perform as frequency filters whose modulation transfer functions are given by the Fourier transform of their response to a modulation impulse. Recirculating delay lines are also of interest for applications requiring short-term storage of discrete or analog signals. In addition to frequency filtering, tapped delay lines can perform a variety of time-domain operations, such as convolution, correlation, and matrix–vector multiplication.

Recirculating and tapped delay lines can be incorporated into basic recursive and nonrecursive fiber-optic structures (Fig. 5(a) and (b)). These basic structures can act as building blocks for more complex forms called *lattice structures*. Lattice structures are capable of performing a wide range of frequency-domain and time-domain filtering operations. Fig. 6(a) and (b) show schematics of two basic lattice forms: the Nth-order feed-backward and feed-forward structures. These configurations are constructed by interconnecting N-recursive sections and N-nonrecursive sections in tandem, respectively. These basic building blocks can allow the application of the classical synthesis

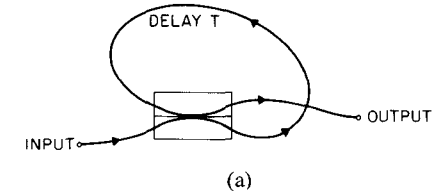

(a)

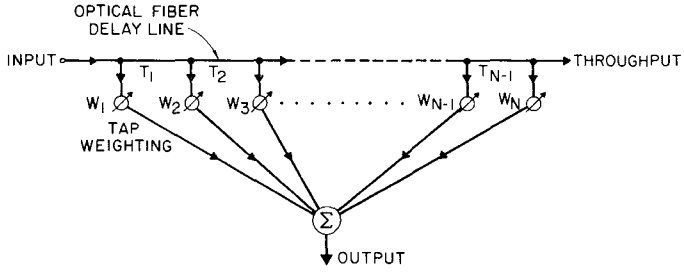

(b)

Fig. 4. Basic delay-line structures: (a) recirculating delay line with loop delay T and (b) tapped delay line with tap intervals T_m ($m = 1,2,\ldots,N-1$) and weighting elements W_m ($m = 0,1,2,\ldots,N$).

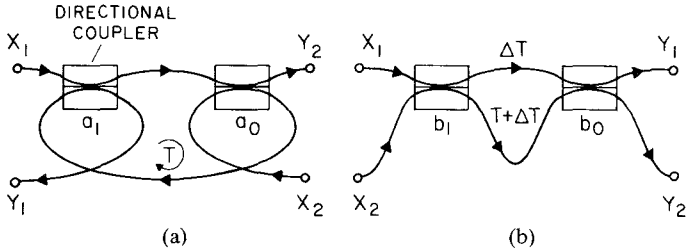

(a) (b)

Fig. 5 Basic recursive and nonrecursive fiber-optic structures: (a) recursive element and (b) nonrecursive element.

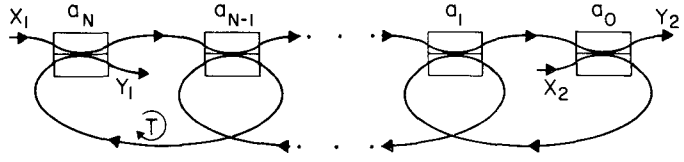

(a)

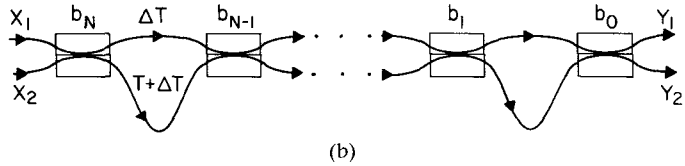

(b)

Fig. 6. Basic lattice forms: (a) Nth-order feed-backward lattice and (b) Nth-order feed-forward lattice.

procedures of lattice filtering to high-frequency fiber-optic filters [27].

This section has discussed some of the factors that must be considered when using optical fiber delay lines for signal-processing applications. While coherent carrier interference can pose a potential problem in fiber delay-line filters, its effects can be greatly reduced by spatial averaging of the tapped light at the detector and by the use of a highly incoherent source.

Also in this section, some of the basic fiber-optic forms that are capable of performing a variety of signal-processing operations have been presented. Given this foundation, the objective of our work has been to implement these structures in the laboratory. The initial effort focussed primarily on methods of tapping optical fibers. Once these tapping mechanisms were identified and implemented, the basic delay-line structures described above were constructed.

In the remaining sections of this paper, three different approaches to implementing basic recirculating and nonrecirculating (tapped) delay lines are described. In each discussion, the design, construction, and performance of these single-mode fiber delay-line devices are presented. In the final section, the lattice structure approach, which combines recirculating and nonrecirculating delay-line sections, is described. Analytical formulations for these structures and the demonstration of elementary processing operations using them is presented.

IV. Optical Fiber Delay-Line Devices

A. The Macrobend Tapped Delay Line

The macrobend tapped delay line is one form of a nonrecirculating delay line. In this device, taps are implemented by forcing a fiber over a series of abrupt bends, causing a small portion of the propagating signal to be radiated at each bend. The device acts as a transversal filter when this radiated light is collected and summed. This tapping technique is particularly attractive because it is nondestructive and noninvasive and can be easily extended to provide for a large number of taps on a single delay line.

Fig. 7 shows the tapping mechanism. When a single-mode optical fiber encounters an abrupt bend, the propagating mode is perturbed and some of the light is emitted in a directional cone. Such a bend can be formed by forcing the fiber over a small pin as shown in Fig. 7. The strength and shape of the radiation pattern depends primarily on the pin radius and its distance from the outer surface of the mandrel.

A macrobend tapped delay line is constructed by wrapping single-mode fiber with a transparent jacket around a mandrel which has a small tapping pin laid at one point along its circumference (Fig. 8). In many of the devices, micrometers have been used as shown in Fig. 8. These micrometers allow the tapping pin to be canted, increasing the fiber tension for later taps and compensating for the delay line and tap attenuation. The portion of the mandrel containing the tapping pin is immersed in a bath of index-matching fluid, which serves to extract that fraction of the light radiated from the core that would otherwise be trapped in the cladding of the fiber. The tapped light is collected by a lens that images the row of taps at an intermediate plane. An encoded transmission mask located in this plane serves to weight the taps by attenuating the light at the image of each tap. The light that is transmitted is collected by a second lens and focused on a detector. In this way, the simultaneous summation of the taps that is needed for transversal filtering is accomplished optically.

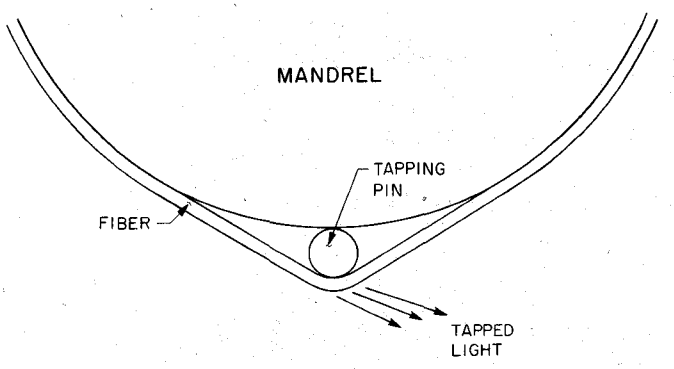

Fig. 7. Schematic diagram illustrating the macrobend tapping mechanism.

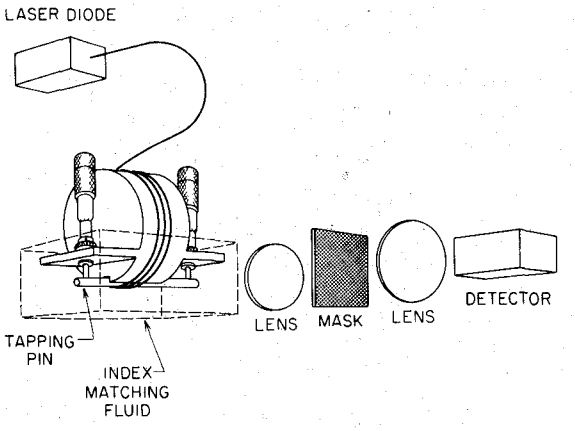

Fig. 8. Schematic diagram of macrobend tapped delay-line transversal filter.

Macrobend delay-line devices have been fabricated as described above. Tapping uniformities are typically ± 1 dB for devices having on the order of twenty taps and about ± 2 dB for devices having on the order of one hundred taps. The tapping uniformity appears to be a function of tension variations during wrapping and variations in the optical quality of the nominally transparent fiber jacket.

The macrobend tapped delay line has been used to generate coded sequences at gigabit/s rates [28]. By injecting into the device an optical pulse which is short compared to the tap spacing, a series of pulses can be generated whose time separations are equal to the tapping interval. A desired coded sequence can be obtained by optically attenuating the desired tapped output signals at the intermediate image plane. Fig. 9 shows two 8-bit coded sequences generated with a device having a 10-cm circumference which corresponds to a 500-ps tapping interval. The uniformity of the pulse amplitudes is better than ± 1 dB.

Convolution and cross-correlation can be performed using a similar arrangement [28]. A modulated optical signal launched into one end of the delay line produces an output at the photodetector which is the convolution of the input signal with the tap weightings. If the tap weights are such that the impulse response is the time-reversed version of the input signal, then the output is the autocorrelation of the input signal and the delay-line device acts as a matched filter.

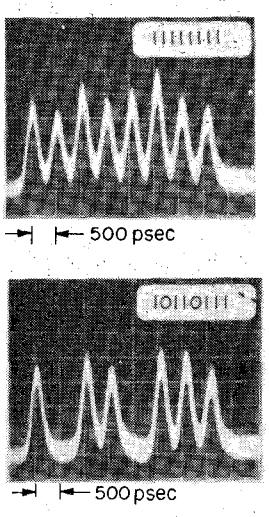

Fig. 9. Eight-bit codes generated with an eight-tap delay line having 500-ps tap intervals.

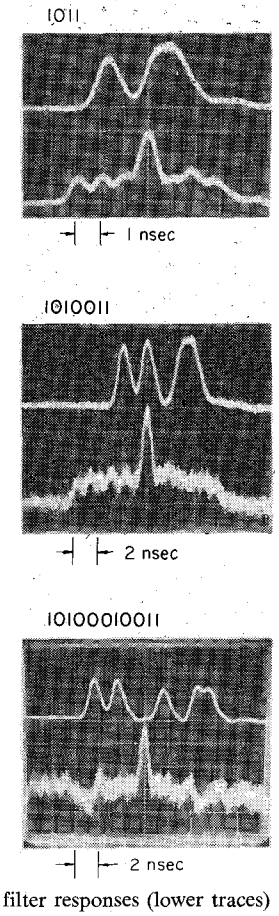

Fig. 10. Matched filter responses (lower traces) to 1 Gb/s input codes (upper traces).

Matched filtering operations have been performed using a device having a 20-cm circumference which corresponds to a 1-ns tapping interval. Fig. 10(a)–(c) show the results for three different on–off codes. These particular codes were chosen because, like Barker codes, their autocorrelation waveforms are characterized by strong central peaks and flat or nearly flat sidelobes. The autocorrelation of the 11-bit code (Fig. 10(c)) is not shown completely in order to resolve the detail near the peak. The features in the response of the 11-bit code are expected, corresponding to a two and zero, which should occur 5 ns on either side of the central peak.

Macrobend tapped delay lines can also perform as frequency filters [29]. The response of a device having 19 taps spaced 1-ns apart was measured at frequencies from 0 to 1.3 GHz. The observed response deviated from the expected $\sin x/x$ response due to variations in tap uniformity. Passbands were located at frequencies corresponding to integer multiples of the inverse of the tap spacing and the widths of each passband were inversely proportional to the number of taps incident on the detector.

Thus far, the macrobend tapped delay-line technique has been demonstrated with devices having relatively small numbers of taps. Larger numbers of taps can be obtained by simply wrapping more fiber turns around the mandrel. The minimum possible tapping interval for these devices is limited by the maximum curvature the fiber can tolerate before significant bending losses occur. For commercially available fiber, bending radii of a few centimeters are possible corresponding to a few hundred picoseconds of delay. Smaller delays may be obtained by tapping the fiber more than once per turn.

B. The V-Groove Tapped Delay Line

The V-groove tapped delay line is an alternative approach to the optical fiber tapped delay line. While lacking the simplicity of the macrobend tapped delay line, this approach offers several important advantages that result from the employment of a more efficient tapping mechanism: the evanescent coupling of two fibers whose cores are in close proximity. This mechanism is implemented using a preferentially etched silicon V-groove substrate to align and position an array of directional coupler taps precisely on a continuous single-mode fiber delay line. By simultaneously summing the individual tap outputs, the device can be used as a transversal filter.

The tapping mechanism of the V-groove device is based on a single-mode directional coupler in which the fiber cladding is removed by mechanical polishing [30]. Each half of a four-terminal directional coupler is made by bonding a fiber in a curved (typically $R = 25$ cm) groove in a quartz substrate (Fig. 11(a)). The surface is first ground, then polished until the fiber cladding is removed to within a few microns of the core.

A directional coupler is formed by mating two identical coupler halves face-to-face, as shown in Fig. 11(b). A thin interfacial layer of index matching oil aids the coupling and allows the substrates to slide smoothly over each other. Maximum coupling occurs when the polished fibers are superposed and the separation between their cores is minimized. Smaller amounts of coupling can be obtained, if desired, by translating one substrate relative to the other, thereby increasing the separation of the fiber cores. In practice, this is accomplished by mounting the coupler in a holder that holds one substrate fixed while a pair of micrometers are used to position the other. In this way, the coupling can be adjusted to a desired value, and if the

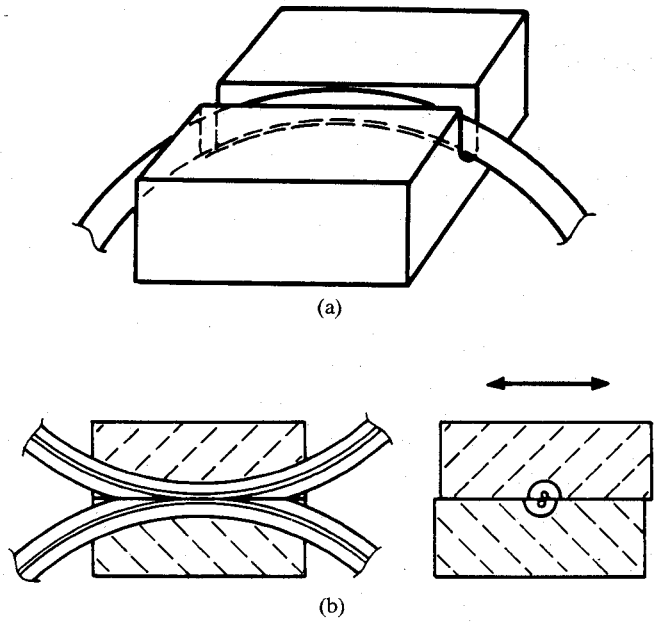

Fig. 11. Single-mode fiber directional coupler: (a) half of a directional coupler and (b) mated halves showing side-view (left) and end-view (right).

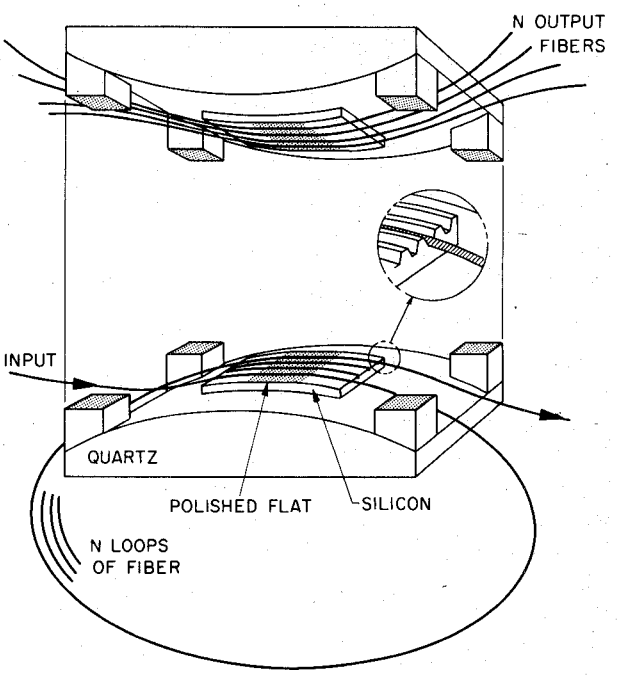

Fig. 12. Exploded view of V-groove tapped delay line.

substrates have been sufficiently polished, full coupling can be achieved.

The single-mode directional coupler exhibits many characteristics that make it highly desirable as a power divider for single-mode fiber devices and systems. The coupler typically exhibits very low excess loss (< 0.5 dB) and is highly directional, with a directivity exceeding 70 dB. The dependence of the coupler on the input polarization is also very small (< 0.1 percent). This fact is important for uniform coupling in the V-groove delay line, where birefringence induced by bends in the fiber changes the state of polarization between each directional coupler tap.

The V-groove tapped delay line is essentially a large number of couplers on a single substrate. The device is made by bonding subsequent turns of a delay-line coil into adjacent grooves of an anisotropically etched silicon V-groove wafer mounted on a curved quartz substrate (Fig. 12). The substrate is mechanically polished in a manner similar to that used for the four-terminal directional coupler mentioned above. A tapped delay line is made by mating this array with a similar array of individual output fibers. The result is an array of evanescently coupled taps. The relative offset of the two arrays at each tap can be adjusted by lateral translation of the entire output array, thus changing the coupling at every tap by the same amount. The uniformity of the core-to-core spacing (and thus the coupling) at each tap site is guaranteed by the precision of the photolithographically processed silicon wafer.

The adjustability, tapping uniformity, and excess tap loss have been measured for a number of V-groove devices [31]. The tapping uniformity of a four-tap device was evaluated for tapping strengths ranging from -10 dB to -50 dB. In all cases, the uniformity was better than ± 1.5 dB. The excess tap loss, which was found to be dependent on the tap strength, was less than 0.26 dB per tap. Devices with larger numbers of taps have also been measured with comparable uniformities and excess losses.

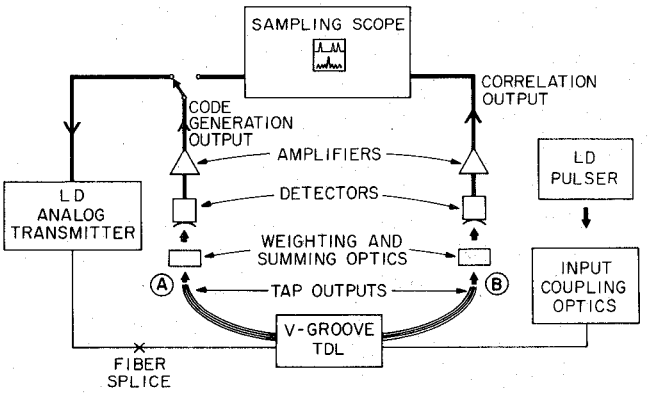

Fig. 13. Experimental arrangement for demonstrating code generation and correlation.

The use of the V-groove tapped delay line as a transversal filter is analogous to that described for the macrobend tapped delay line [26]. The experimental arrangement for both code generation and correlation using the V-groove device is shown schematically in Fig. 13. In this arrangement, coded sequences are generated by injecting a short optical pulse into the right-hand end of the delay line. The tapped outputs emerge at location A (Fig. 13) where they are weighted and optically summed by combining them on a single detector.

Closed-loop correlation has been performed by using the LD analog transmitter to reinject the generated sequence into the other (left-hand) end of the delay line. This sequence is then sampled, weighted, and again combined onto a single detector (Output B, Fig. 13). The result, in this instance, is the cross-correlation of the tap weightings at Output A with the tap weightings at Output B.

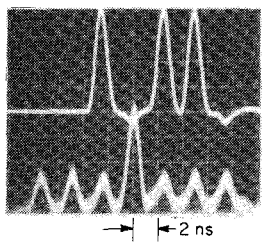

Fig. 14. V-groove tapped delay-line correlator. Coded sequence generation (upper trace) and autocorrelation (lower trace) of 1011.

Fig. 14 shows an experimental closed-loop result obtained with a four-tap device having 2.5-ns tapping intervals. The code 1011 in the upper trace was generated by a single input pulse from the pulser with weightings at tap Output A. The correlation output (lower trace) was obtained by feeding the output from A to the analog transmitter and injecting its optical output into the left-hand end of the delay line. Since the weightings at Output B were adjusted to be the same as those of Output A, the output of the detector at B is the autocorrelation of the generated sequence.

A V-groove tapped delay line can also perform as a frequency filter that responds selectively to different modulation frequencies. Fig. 15(a)–(c) shows measured frequency responses for a four-tap device with equally weighted taps (2.5-ns tapping intervals). The sequence of photographs illustrate the dependence of the width of the fundamental passband on the number of unmasked taps incident on the detector.

The V-groove tapped delay line is capable of performing other processing operations. For example, a V-groove device has been demonstrated as a discretely variable delay line [32]. Frequency- and time-domain measurements were carried out on a device with adjustable delays ranging from 0.6 ns to 14.4 ns.

The V-groove tapped delay line has proven to be a versatile device that exhibits important advantages as a tapped delay line. Its major advantage lies in the fact that the tapped light can be efficiently collected and transported from the delay line by single-mode fibers. As a result, the tap outputs can potentially be recombined in a solitary single-mode fiber using a similar set of V-groove arrays. This procedure can be beneficial, since high-speed detectors necessarily have small sensitive areas, and collection of the tapped light in a single fiber whose output falls within this small area without focusing is essential for the efficient detection of large numbers of tap outputs.

Finally, the V-groove tapped delay line can have tap intervals that are extremely small. Like the macrobend tapped delay line, the physical spacing of the taps on the V-groove delay-line coil is limited by bending losses to several millimeters, corresponding to an interval of a few hundred picoseconds. The effective tap interval can be much shorter, however, since extra delay can be provided by the fibers that guide the tap outputs to the summing point. This interval may be as small as the interaction length of a directional coupler or the coherence time of the optical source, whichever is larger.

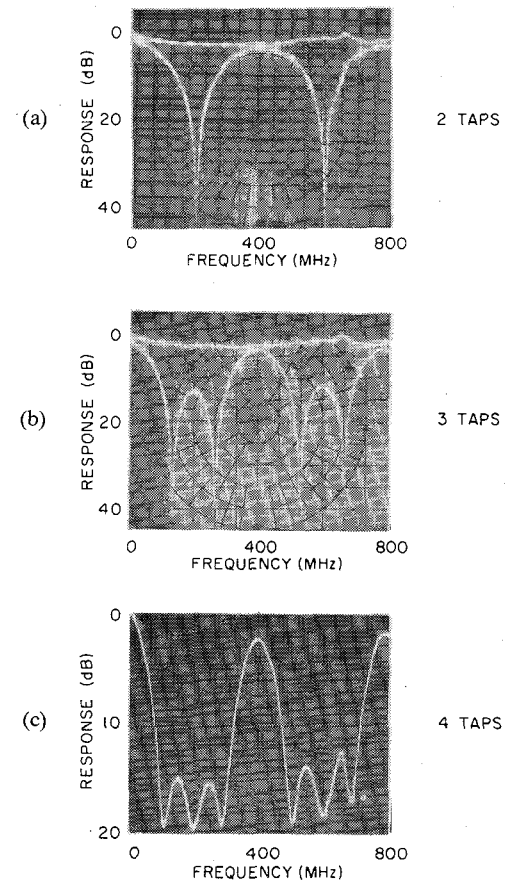

Fig. 15. Frequency response of V-groove filter using (a) two taps, (b) three taps, and (c) four taps. Upper trace in (a) and (b) is the frequency response of the measurement system.

C. The Recirculating Delay Line

The recirculating delay line is formed using the single-mode directional coupler discussed earlier. The loop can be formed without a splice by appropriately mating two coupler halves that have been fabricated on a single strand of fiber (Fig. 4(a)). The resulting directional coupler tap allows signals to be launched into the loop as well as to be extracted from it. The amount of recirculation in the delay-line loop is determined by the coupling coefficient, the excess loss of the coupler, and the propagation loss in the fiber loop.

An important class of time-domain applications exist wherein fiber recirculating delay lines can be used for data-rate transformations [33]. A recirculating loop can be used as a buffer memory that will accept information at a given data rate, temporarily store it, and transmit it at a different rate. For example, such a device would allow the interfacing of a sensor that is acquiring and transmitting information at one rate to a processor that requires the entry of data at a different rate.

In the "slow in–fast out" mode (Fig. 16(a)), a slow stream of data pulses (rate $1/T$) is injected into a loop having a circulation transit time $T-\tau$. In this way, each pulse is injected a time τ after the previous pulse has completed a full circulation. Thus, the pulses are interleaved such that they are separated by τ as they circulate in

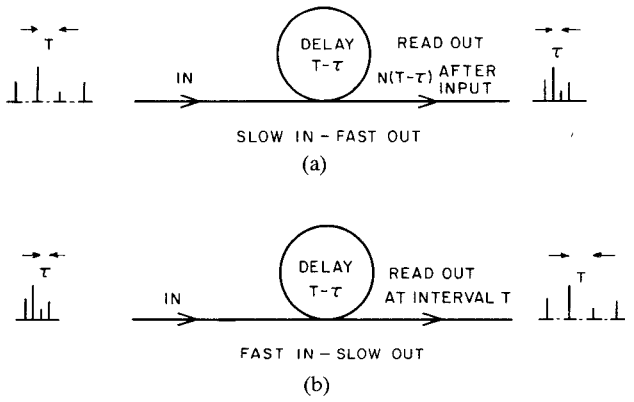

Fig. 16. Data-rate transformations using a recirculating delay line. (a) Slow in–fast out. (b) Fast in–slow out.

the loop. Once the entire pulse stream has been read into the loop, it can be read out at a bit rate of $1/\tau$.

In the "fast in–slow out" mode (Fig. 16(b)), a high-speed data stream is injected directly into a loop, which also has transit time $T-\tau$. Individual pulses can then be read out one by one at a regular interval T until the entire code is recovered at the slower rate $1/T$.

In practice, both of these transformer modes require amplification to compensate propagation and coupling loss, as well as switchable, gated coupling to selectively inject or extract individual pulses or groups of pulses. While the "slow in–fast out" mode requires a relatively slow gate with a switching time on the order of T, the "fast in–slow out" mode requires a fast gate with a switching time less than τ in order to extract individual pulses from a circulating high-speed pulse train.

One interesting application, which demonstrates the potential of recirculating delay lines to performing data-rate transformations, is uniform pulse-train generation [34]. In this application, two single-mode fiber recirculating delay lines are used in series to generate a sequence of uniform pulse trains (Fig. 17). When a single short pulse is launched into a "generator" loop having transit time T, the output consists of an infinite, decaying series of pulses spaced by T. If such a sequence is coupled into a "multiplexer" loop having transit time $T-\tau$, then each pulse of the input sequence enters the loop a time τ after the previous pulse has completed a full circulation. The circulating pulses in the multiplexer loop are thus spaced by τ, and are sampled by the coupler on each pass and transmitted to the output. The Nth pulse train of the output sequence is composed of N pulses with each pulse making a total of $N-1$ circulations in the generator loop, the multiplexer loop, or some combination of the two. As a result, if the coupling and loss parameters of the multiplexer loop are identical to those of the generator loop, the pulses within each pulse train will be uniform.

This concept was demonstrated experimentally by injecting a short (120 ps FWHM) pulse from a laser diode ($\lambda = 820$ nm) into a generator loop having a transit time of 10.9 ns. The output of the generator loop then entered a multiplexer loop having a transit time of 10.1 ns. The coupling and loss parameters were adjusted to be equal in

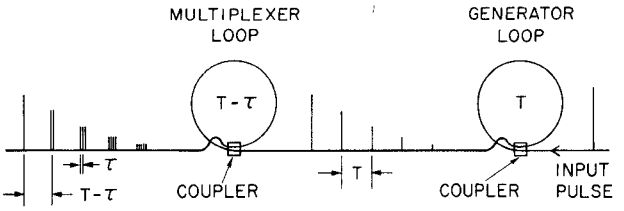

Fig. 17. Schematic diagram illustrating pulse-train generation with recirculating delay lines.

both loops with the adjustable directional couplers and variable splices within each loop, respectively. The resulting output (Fig. 18) consisted of a sequence of 1.25 Gb/s (corresponding to a 0.8-ns difference in loop transits) pulses with pulse heights within a given pulse train uniform to better than ± 0.3 dB.

This technique provides a simple method for generating a series of high-speed uniform pulses. Since the interval τ between pulses within each pulse train depends only on the transit time difference between the generator and multiplexer loops, this interval may be extremely short, limited only by the width of the original input pulse. The interval between pulse trains may be much longer, however, enabling the extraction of a desired pulse train from the series by a relatively slow gate. In order to extract the Nth pulse train from the output sequence, the switching time of the gate needs to be only $T-N\tau$.

Recirculating delay lines can also be used for frequency filtering. The frequency response depends on the adjustment of the coupler, the propagation loss of the loop, and the insertion loss of the coupler. Notch filtering has been demonstrated using a variety of recirculating delay lines with loop delays ranging from 1.00 μs to 1.35 ns [35]. The frequency responses were characterized by having deep notches (-55 dB) and uniform overtones extending beyond one gigahertz. The uniformity of these overtones was limited by the measurement system (laser diode, detector, amplifier, and network analyzer) and therefore the response of these fiber filters should be uniform well beyond several tens of gigahertz.

This property was investigated using a microwave measurement system [36] which included a lithium niobate waveguide modulator [37], a high-speed GaAs photodetector [38], a spectrum analyzer, and a sweep oscillator (Fig. 19). The output from a CW laser diode ($\lambda = 820$ nm) was focused into the waveguide modulator which was driven over a broad frequency range by the sweep oscillator. The modulated light output was coupled into a fiber filter (1.35-ns loop delay) which after passing through the filter was detected by the GaAs photodetector. The output of the photodetector was in turn fed into the spectrum analyzer. The oscillator and spectrum analyzer were stepped together in 10-MHz intervals from 1 to 18 GHz by a desktop computer.

The frequency response of the filter was first measured with the coupler adjusted for maximum notch depth. The loop was then disassembled by separating the coupler halves so that the fiber served as a link (total length 1 m) from the modulator to the detector. Since the modulation

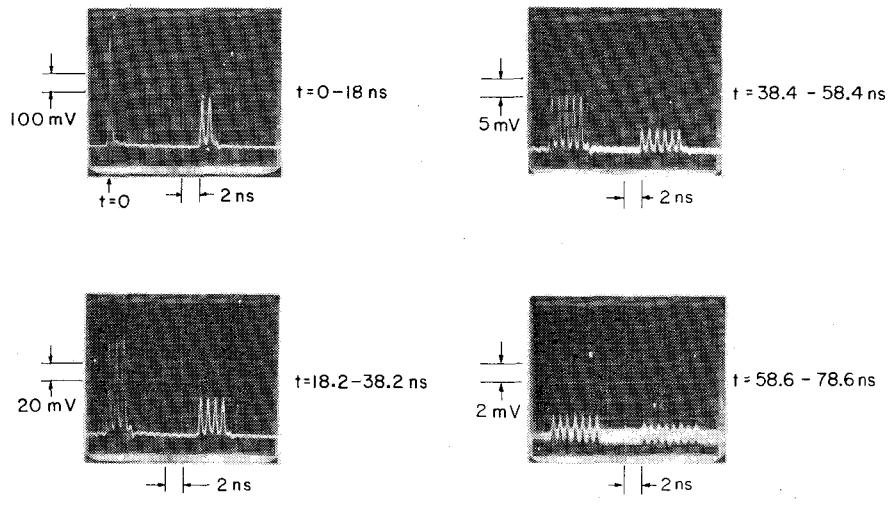

Fig. 18. Pulse-train output sequence of multiplexer loop.

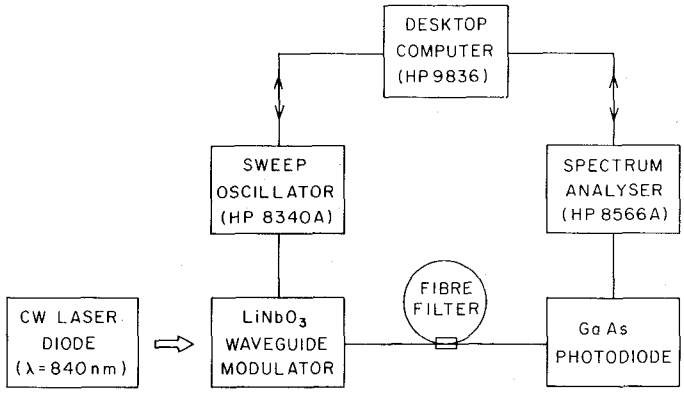

Fig. 19. Experimental arrangement for measuring microwave frequency response of fiber filter.

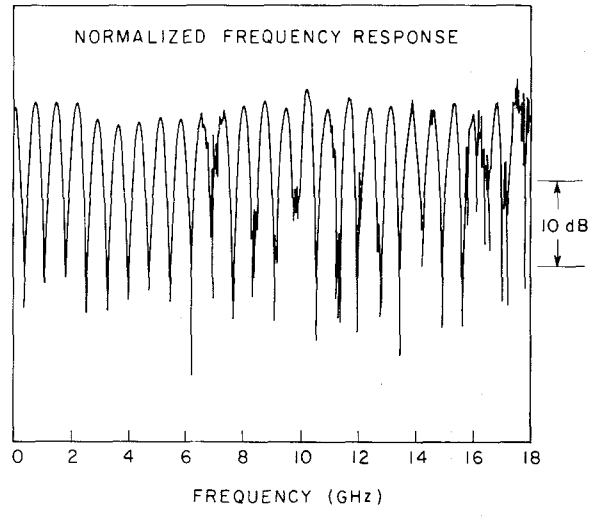

Fig. 20. Normalized frequency response of notch filter from 0–18 GHz.

bandwidth of this length of single-mode fiber is on the order of 1 THz, the measurement yields the residual frequency response of the measurement system. This response was then used to normalize the response measured with the recirculating delay line included in the system. The response illustrated in Fig. 20 contains sharp notches at the appropriate frequencies, ranging in depth from -12 dB to -30 dB. The notch depth was limited by receiver noise and by deviation of the coupling coefficient from the desired value. The filter exhibited a fundamental passband at 740 MHz with overtones that are uniform to within ± 1.5 dB to at least 18 GHz, at which point their measurement was limited by the dynamic range of the system. It is worth noting that this uniformity is better than the specified flatness uncertainty of the spectrum analyzer.

Recirculating delay lines are capable of providing other processing functions such as bandpass filtering. As before, the response of these filters can be tailored by adjustment of the coupling coefficient. Analyses and experimental results of these filtering operations are contained in [35].

The recirculating delay-line structures developed thus far have loop delays that are of modest lengths due to limitations imposed by the measurement systems. Ultimately, recirculating delay lines can provide much shorter delays. The shortest possible loop delay is limited by bending losses to a minimum circumference corresponding to a circulation time of a few hundred picoseconds. Greater versatility of the recirculating delay line in both time- and frequency-domain applications will depend in a large part on the development of additional components. For example, an in-line optical amplifier capable of boosting broadband signals with a minimum of distortion and excess noise would be advantageous. Such an internal device may need only to provide a few decibels of gain to compensate the coupler and fiber loss. In addition to an amplifier, the use of a rapidly switchable directional coupler would greatly enhance the performance of these devices. An increase in signal-to-noise ratio could be realized if the coupling could be switched at desired instants so that circulating signals would not be significantly depleted prior to their extraction.

D. Lattice Structures

Fiber-optic lattice structures have been developed using directional couplers. Recursive or nonrecursive fiber-optic sections are formed by appropriately orienting the mated halves of the directional couplers (Fig. 5(a) and (b)). More

complicated structures such as a feed-forward or feed-backward lattice can be implemented by cascading these elementary recursive and nonrecursive sections (Fig. 6(a) and (b)). A thorough analysis of fiber lattice structures including experimental results is presented in [27]. Therefore, only the significant features and experimental results will be presented here.

Lattice structures can be used to perform a variety of time-domain signal processing operations, including code generation, convolution, and correlation. These operations can be performed using feed-forward or feed-backward fiber lattices. One interesting area of time-domain application, which is well suited for the lattice structure approach, is that of matrix–vector operations. In this application, a feed-backward fiber structure (Fig. 6(a)) is used to implement a matrix processor capable of performing high-speed matrix–vector multiplications. The clock rate of this processor is set by the basic loop delay of the elementary recursive sections that form the feed-backward structure. The operation of the multiplier involves $2N-1$ couplers, corresponding to the $2N-1$ main and off diagonals of a given $N \times N$ matrix. As the components of the input vector are serially fed as optical signals into the input line X_1 of Fig. 6(a), the matrix elements enter the couplers progressively in such a way that each coupling coefficient represents matrix elements from a single off (or main) diagonal.

This arrangement uses couplers which presently are adjusted manually. As a result, multiplications involving only Toeplitz matrices (i.e., matrices in which all the elements along each diagonal are equal) can be performed. Toeplitz matrices can be utilized to represent many important signal-processing operations including convolution, correlation, and Fourier transformation. With the introduction of fast switchable couplers, however, general matrix operations could be performed and the versatility of these processors would be greatly expanded.

The operation of the matrix multiplier with fixed weights is described in Fig. 21 for a 2×2 Toeplitz matrix. The matrix elements are represented by the coupling coefficients (a_i), which are assumed to be sufficiently weak so that the input vector is not significantly attenuated by the couplers and that additional recirculations are negligible. The components of the input vector enter the input line as a time sequence of light pulses whose spacings are equal to the round-trip loop delay T between adjacent couplers. Since the device is linear in the intensity of the propagating light, the total response of the output is the sum of the responses to the two components of the input vector. As illustrated in Fig. 21, the matrix–vector product appears in a time slot of width two unit time delays following the first pulse. A similar result holds for the general (Toeplitz) N-dimensional matrix–vector multiplication. For such a matrix, $2N-1$ couplers would be required and the N components of the output vector would follow the $(N-1)$th output pulse.

An experimental device was built from three directional couplers with a basic loop delay of 10 ns which corresponds to a 100-MHz clock rate. The three couplers were manually adjusted to yield an impulse response with the first three pulse heights proportional to a_{12}, $a_{11}(=a_{22})$, and a_{22}, respectively. The experimental output vectors, which are shown in Fig. 22(a) and (b), follow theoretical predictions.

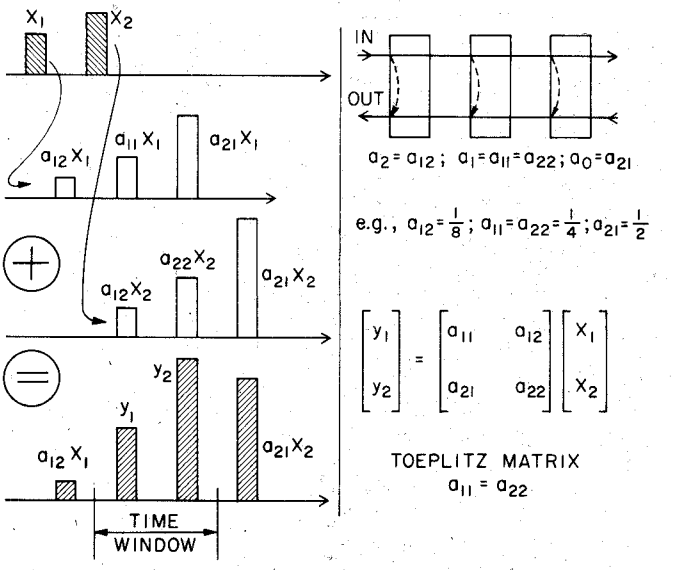

Fig. 21. Systolic Toeplitz matrix–vector multiplier for 2×2 matrices. $[A_i]$ are the coupling ratios of the three couplers. The output is the sum of the contributions made by each of the vector components.

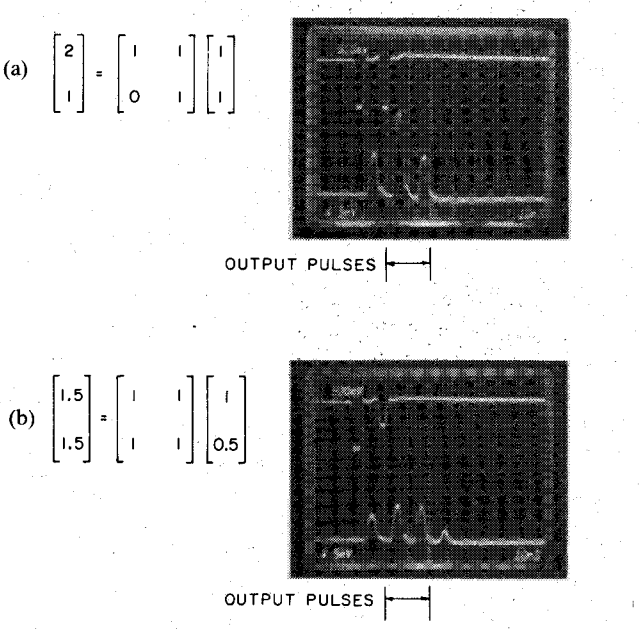

Fig. 22. Experimental matrix–vector products (arbitrary vertical scales). The upper traces show the electronic input pulses. The undershoots that follow the pulses result from the high-pass characteristics of the electronic circuitry.

Among the factors that may determine the ultimate accuracy of the multiplier are the settings of the coupling coefficients, the time delay between the input pulses, the loop delays, the presence of residual recirculations (for high-data rate applications), and the frequency bandwidth of the electronic components. It should be noted that by incorporating smaller fiber loops (few centimeters) and

designing smaller components and a more compact geometry, the effective clock rate of these devices can be extended to several gigahertz. Also, higher order lattices can be used to operate on matrices of higher dimension. This extension only requires additional lengths of fiber and couplers.

Lattice structures are also important in frequency-domain operations. A variety of filter responses can be realized by combining lattice sections in prescribed ways. The analysis of fiber lattices can be conveniently carried out by representing the structures with a system response matrix and using Z-transform techniques. Each elementary recursive or nonrecursive section can be represented by a matrix whose elements relate the input and output terminals of the section. For example, the elementary two-coupler nonrecursive section can be described by a *transfer matrix*, which relates the first port with input terminals X_1 and X_2 to the second port with output terminals Y_1 and Y_2 (Fig. 5(b)) [27]

$$H=\begin{pmatrix} H_{11}(z) & H_{12}(z) \\ H_{21}(z) & H_{22}(z) \end{pmatrix} \tag{5}$$

where

$$\begin{cases} H_{11}=(1-b_1)(1-b_0)l_{11}+b_1b_0l_{12}z^{-1} \\ H_{12}=b_1(1-b_0)l_{11}+(1-b_1)b_0l_{12}z^{-1} \\ H_{21}=(1-b_1)b_0l_{11}+b_1(1-b_0)l_{12}z^{-1} \\ H_{22}=b_1b_0l_{11}+(1-b_1)(1-b_0)l_{12}z^{-1}. \end{cases}$$

l_{11} and l_{12} are the intensity transmission factors from X_1 to Y_1 and X_2 to Y_2, respectively. b_0 and b_1 are the coupling coefficients of the couplers as shown in the figure. z is the Z-transform variable.

A similar matrix representation can be used for two-coupler recursive systems. In these structures, a *chain matrix*, whose elements relate the pairs of input–output terminals (X_1, Y_1) to (X_2, Y_2) (Fig. 5(a)) is used[27]

$$G=\frac{1}{l_{11}(1-a_1)(1-a_0)}\cdot\begin{pmatrix} G_{11}(z) & G_{21}(z) \\ G_{12}(z) & G_{22}(z) \end{pmatrix} \tag{6}$$

where

$$\begin{cases} G_{11}=1-a_1a_0l_1z^{-1} \\ G_{12}=-a_0-a_1(1-2a_0)l_1z^{-1} \\ G_{21}=a_1+(1-2a_1)a_0l_1z^{-1} \\ G_{22}=-a_1a_0+(1-2a_1)(1-2a_0)l_1z^{-1} \end{cases}$$

and $l_1=l_{11}l_{12}$ and a_0 and a_1 are the coupling coefficients of the couplers.

Matrix representations for cascaded systems can be determined in a straightforward manner. For cascaded recursive sections, the system matrix G_{total} is the product of the individual chain matrices, multiplied in the same order as the sections are cascaded, i.e.,

$$G_{\text{total}}=G_1G_2G_3\cdots G_N. \tag{7}$$

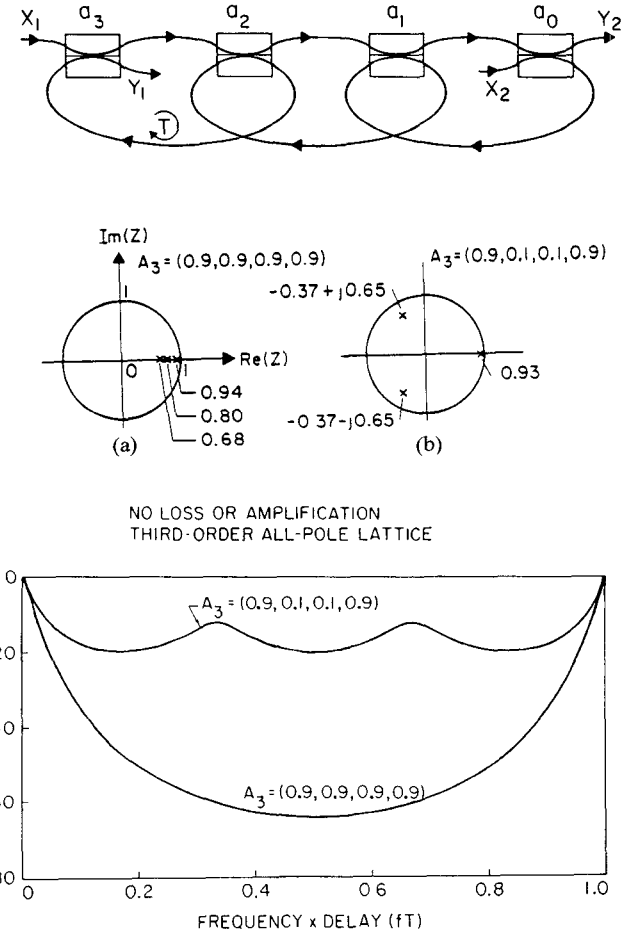

Fig. 23. Theoretical pole diagrams and corresponding frequency responses for a third-order all-pole fiber-optic lattice filter (input port X_1, output port Y_2) for two different values of the coupling coefficient vector (shown in the figure). The coupling coefficient vector A_3 is defined as (a_0, a_1, a_2, a_3).

The same multiplicative rule, but with the reverse order, is valid for the transfer matrices of cascaded nonrecursive sections

$$H_{\text{total}}=H_N\cdots H_3H_2H_1. \tag{8}$$

The elements of a chain matrix can be related to the elements of the corresponding transfer matrix. In this way, matrix representations of systems composed of both recursive and nonrecursive sections can be easily determined.

Theoretical frequency responses for a third-order all-pole lattice are shown in Fig. 23 for two different settings of coupling coefficients. The values of the coupling coefficients are chosen such that for one case all the poles of the corresponding filter transfer function are (real) positive (Fig. 23(a)), and for the other case there are both real and complex poles (Fig. 23(b)). The presence of the two peaks within one basic period of the frequency response (upper curve) is indicative of the existence of complex conjugate pole pairs. In both responses, the peaks at integer multiples of fT correspond to positive-valued poles.

Experimental frequency responses of a second-order feed-backward lattice are shown in Fig. 24(a)–(c). The magnitude of the frequency response shown in Fig. 24(a) was measured with the last coupler in the cascade set to a

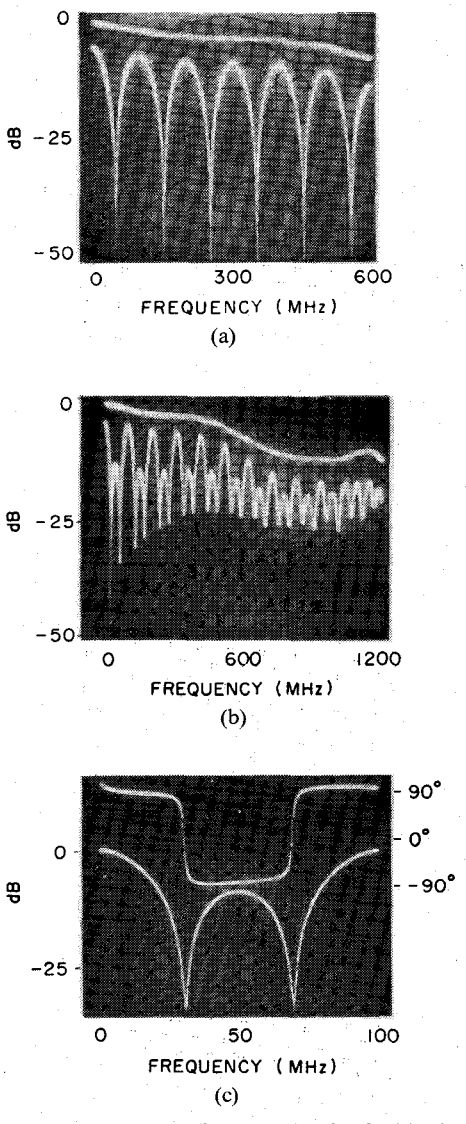

Fig. 24. Frequency responses of a second-order feed-backward lattice with different coupler settings. (a) Response with last coupler in cascade set to zero coupling ratio. (b) Response with coupling ratios set to intermediate values. (c) Expanded portion of the response shown in (b) including phase. Upper traces in (a) and (b) are the frequency responses of the measurement system.

coupling ratio of zero. As a result, the device becomes a first-order filter, and thus only one peak per basic period in the frequency response is observed. Fig. 24(b) shows the frequency response of the lattice with the coupling coefficients set to intermediate values. Fig. 24(c) is an expanded portion of one basic period of the same response including the phase. For these coupling ratios, two peaks per basic period are evident, indicating that the lattice is performing as a second-order filter. The upper traces in Fig. 24(a) and (b) are the responses of the measurement system (i.e., laser diode, detector, and amplifier).

Fiber lattice structures have several advantages that make them attractive for performing many signal-processing functions. For example, the outputs of the structures are contained in a single fiber facilitating the detection process. Also, all summations are done optically, within the fiber, making the systems more efficient. The modular construction of fiber lattices simplifies the design and fabrication of complicated filtering systems. Furthermore, the analysis of these complicated systems is easy since the overall response can be obtained by cascading the responses of elementary sections.

More versatile filters can be constructed by combining feed-forward (all-zero) and all-pole type feed-backward filters. Such an arrangement allows independent adjustment of the poles and zeroes in the Z-plane. As a result, a variety of complex filters can be synthesized. Moreover, combining feed-backward sections with feed-forward sections allowing negativity (e.g., by using the negative detection arrangement described in Section III) can provide even more versatile systems. These combinations can also be analyzed using the formalisms described above.

V. Summary and Future Directions

The objectives of the research reviewed in this paper were to identify and study efficient tapping mechanisms for single-mode fiber delay lines, to develop fabrication techniques that allowed the implementation of these mechanisms, and to construct and test fiber delay-line filters capable of performing some basic signal-processing functions. These objectives were accomplished through the development of three different prototypes: the macrobend tapped delay line, the V-groove tapped delay line, and the recirculating delay line [39]. These prototypes in turn provided the foundation for the development of fiber lattices, which are capable of performing more complicated signal-processing operations [40]. The results obtained with these devices clearly demonstrate the feasibility of fiber delay lines for broad-band signal processing.

The tapped delay-line structures (macrobend and V-groove) have been used to perform basic transversal filtering operations at frequencies of several hundred megahertz to well over a gigahertz. Recirculating delay lines have been used to demonstrate temporary storage of broad-band signals in addition to performing data-rate transformations. Recirculating delay lines have also been demonstrated as frequency filters with measured frequency responses extending beyond a gigahertz. The general synthesis of fiber-optic lattice structures has been explored both theoretically and experimentally. Fiber lattices have been used to perform high-speed matrix operations with clock rates of 100 MHz, as well as broad-band frequency filtering at frequencies over a gigahertz. All of these devices have been demonstrated experimentally at relatively low frequencies but the extension of these techniques to frequencies well above 10 GHz is straightforward. The extension will in most cases involve shorter fiber lengths and more compact designs as well as faster sources and detectors.

The work presented in this paper suggests further research and development that may lead in a number of different directions. Perhaps the most obvious and immediate of these directions is the further engineering and refinement of the existing prototype devices, in order to expand their capabilities. For example, the macrobend and V-groove tapped delay lines will benefit greatly from im-

provements such as the implementation of large numbers of closely spaced taps with the capability of bipolar tap weightings. Innovations such as chirped tap spacings [41] would improve the pulse compression capabilities of these fiber transversal filters significantly. The implementation of electronically programmable tap weights (using a liquid crystal transmission mask, for example) will be of value for both of these devices. Further development of the recirculating delay line depends largely on the availability of new components such as a fast switchable coupling element and an in-line optical amplifier [42]. The versatility of fiber lattices would also be expanded greatly by the development of such components.

Finally, the advantages of fiber delay lines are not limited to their use in the kinds of structures that are encountered in more traditional delay-line technologies. Other areas of application may exist which will benefit from the unique features of optical fiber delay lines, such as their precision timing capabilities and enormous transmission bandwidth. The utility of single-mode fiber delay-line devices for both these and more traditional kinds of high-speed applications is presently limited only by our ability to generate and detect the required optical signals, and this ability is improving rapidly [43]–[45]. Rapid progress in the fields of fiber communication and fiber sensing should insure the further development of components that can be used to exploit the excellent delay properties of single-mode fiber.

ACKNOWLEDGMENT

The authors wish to thank W. V. Sorin and E. Desurvire for helpful discussions and J. L. Brooks for reading this manuscript.

REFERENCES

[1] I. Garrett, "Towards the fundamental limits of optical-fiber communications," *IEEE J. Lightwave Tech.*, vol. LT-1, p. 131, 1983.
[2] T. G. Giallorenzi, J. A. Bucaro, A. Dandridge, G. H. Sigel, Jr., J. H. Cole, S. C. Rashleigh, and R. G. Priest, "Optical fiber sensor technology," *IEEE J. Quantum Electron.*, vol. QE-18, p. 626, 1982.
[3] K. Ogawa, "Considerations for single mode fiber systems," *Bell Syst. Tech. J.*, vol. 61, p. 1919, 1982.
[4] P. D. Lazay and A. D. Pearson, "Developments in single-mode fiber design, materials, and performance at Bell Laboratories," *IEEE J. Quantum Electron.*, vol. QE-18, p. 504, 1982.
[5] D. D. Buss, R. W. Broderson, and C. R. Hewes, "Charge-coupled devices for analog signal processing," *Proc. IEEE*, vol. 64, p. 801, 1976.
[6] W. P. Mason, "Multiple reflection ultrasonic delay lines," in *Physical Acoustics*, vol. 1. New York: Academic, p. 485, 1964.
[7] J E. May, "Guided wave ultrasonic delay lines," in *Physical Acoustics*, vol. 1. New York: Academic, p. 417, 1964.
[8] G. D. Boyd, L. A. Coldren, and R. N. Thurston, "Acoustic waveguide with a cladded core geometry," *Appl. Phys. Lett.*, vol. 26, 31 1975.
[9] L. T Claiborne, G. S. Kino, and E. Stern, Eds., "Special Issue on Surface Acoustic Waves," *Proc. IEEE*, vol. 64, 1976.
[10] J. D Adam and M. R. Daniel, "The status of magnetostatic devices," *IEEE Trans. Mag.*, vol. MAG-17, p. 2951, 1981.
[11] S. A. Reible, "Wideband analog signal processing with superconductive circuits," in *IEEE Proc. Ultrasonics Symp.*, vol. 1, 1982, p. 190.
[12] J. T. Lynch, R. S. Withers, A. C. Anderson, P. V Wright, and S. A. Reible, "Multigigahertz-bandwidth linear-frequency-modulated filters using a superconductive stripline," *Appl. Phys. Lett.*, vol. 43, p. 319, 1983.
[13] K. Wilner and A. P. van den Heuvel, "Fiber-optic delay lines for microwave signal processing," *Proc. IEEE*, vol. 64, p. 805, 1976.
[14] R. L. Ohlhaber and K. Wilner, "Fiber optic delay lines for pulse coding," *Electro-optical Syst. Des.*, vol. 9, p. 33, 1977.
[15] C. T. Chang, J. A. Cassaboom, and H. F. Taylor, "Fibre-optic delay-line devices for R.F. signal processing," *Electron. Lett.*, vol. 13, p. 678, 1977.
[16] H. F. Taylor, "Fiber and integrated optical devices for signal processing," *Proc. SPIE*, vol. 176, p. 17, 1979.
[17] E. O. Rausch, R. B. Efurd, and M. A. Corbin, "A fiber optic pulse compression device for high resolution radars," presented at *Inst. Elec. Eng. Int. Conf. Radar*, 1982.
[18] D. A. Pinnow, T. C. Rich, F. W. Ostermayer, Jr., and M. DiDomenico, Jr., "Fundamental optical attenuation limits in the liquid and glassy state with application to fiber optical waveguide materials," *Appl. Phys. Lett.*, vol. 22, p. 527, 1973.
[19] J. E. Midwinter, *Optical Fibers for Transmission*. New York: Wiley, 1979.
[20] Donald B. Keck, "Single-mode fibers outperform multimode cables," *IEEE Spectrum*, vol. 20, p. 30, 1983.
[21] K. Ogawa, "Considerations for single mode fiber systems," *Bell Syst. Tech. J.*, vol. 61, p. 1919, 1982.
[22] D. Marcuse, *Principles of Quantum Electronics*. New York: Academic, 1980.
[23] R. G. Smith, "Optical power handling capacity of low loss optical fibers as determined by stimulated Raman and Brillouin scattering," *Appl. Opt.*, vol. 11, p. 2489, 1972.
[24] W. D. Johnston, Jr., I. P. Kaminow, and J. G. Bergman, Jr., "Stimulated Raman gain coefficients for Li^6NbO_3, $Ba_2NaNb_5O_{15}$, and other materials," *Appl. Phys. Lett.*, vol. 13, p. 190, 1968.
[25] J. W. Goodman, A. R. Dias, L. M. Woody, and J. Erickson, "Application of optical communication technology to optical information processing," *Proc. SPIE*, vol. 190, pp. 485–496, 1979.
[26] S. A. Newton, K. P. Jackson, H. J. Shaw, "Optical fiber V-groove transversal filter," *Appl. Phys. Lett.*, vol. 43, p. 149, 1983.
[27] B. Moslehi, J. W. Goodman, M. Tur, and H. J. Shaw, "Fiber-optic lattice signal processing," *Proc. IEEE*, vol. 72, p. 909, 1984.
[28] K. P. Jackson, S. A. Newton, and H. J. Shaw, "1-Gbit/s code generator and matched filter using an optical fiber tapped delay line," *Appl. Phys. Lett.*, vol. 42, p. 556, 1983.
[29] K. P. Jackson, J. E. Bowers, S. A. Newton, and C. C. Cutler, "Microbend optical fiber tapped delay line for gigahertz signal processing," *Appl. Phys. Lett.*, vol. 41, p. 139, 1982.
[30] R. A. Bergh, G. Kotler, and H. J. Shaw, "Single-mode fiber-optic directional coupler," *Electron. Lett.*, vol. 16, p. 260, 1980.
[31] S. A. Newton, J. E. Bowers, G. Kotler, and H. J. Shaw, "Single-mode-fiber $1 \times N$ directional coupler," *Opt. Lett.*, vol. 8, p. 60, 1983.
[32] J. E. Bowers, S. A. Newton, and H. J. Shaw, "Fibre-optic variable delay lines," *Electron. Lett.*, vol. 18, p. 999, 1982.
[33] S. A. Newton, J. E. Bowers, and H. J. Shaw, "Single mode fiber recirculating delay line," *Proc. SPIE*, vol. 326, p. 108, 1982.
[34] S. A. Newton, R. S. Howland, K. P. Jackson, and H. J. Shaw, "High-speed pulse-train generation using single-mode fibre recirculating delay lines," *Electron. Lett.*, vol. 19, p. 756, 1983.
[35] J. E. Bowers, S. A. Newton, W. V. Sorin, and H J. Shaw, "Filter response of single-mode-fibre recirculating delay lines," *Electron. Lett.*, vol. 18, p. 110, 1980.
[36] S. A. Newton and P. S. Cross, "Microwave frequency response of an optical fibre delay line filter," *Electron. Lett.*, vol. 19, p. 480, 1983.
[37] P. S. Cross, R. A. Baumgartner, and B H. Kolner, "Microwave integrated optical modulator," *Appl. Phys. Lett.*, vol. 44, p. 486, 1984.
[38] S. Y. Wang, D. M. Bloom, and D. M. Collins, "20 GHz bandwidth GaAs photodiode," *Appl. Phys. Lett.*, vol. 42, p. 190, 1983.
[39] S. A. Newton, "Optical fiber delay line signal processing," *Edward L. Ginzton Lab.*, Rep. No. 3674, 1984.
[40] B. Moslehi, "Fiber-optic lattice signal processing," *Edward L. Ginzton Lab.*, Rep. No. 3755, 1984.
[41] K. P. Jackson, S. A. Newton, and H. J. Shaw, "Improved macrobend optical-fiber tapped delay line for high-speed signal processing," in *Proc. Optical Fiber Communications (OFC) Conf.*, 1984.
[42] W. V. Sorin, K. P. Jackson, and H. J. Shaw, "Evanescent amplification in a single-mode optical fibre," *Electron. Lett.*, vol. 19, p. 820, 1983.

[43] S. Y. Wang and D. M. Bloom, "100 GHz bandwidth planar GaAs Schottky photodiode," *Electron. Lett.*, vo. 19, p. 554, 1983.
[44] K. Y. Lau, N. Bar-Chaim, I. Ury, Ch. Harder, and A. Yariv, "Direct amplitude modulation of short-cavity GaAs lasers up to *X*-band frequencies," *Appl. Phys. Lett.*, vol. 43, p. 1, 1983.
[45] C. M. Gee, G. D. Thrumond, and H. W. Yen, "17-GHz bandwidth electro-optic modulator," *Appl. Phys. Lett.*, vol. 43, p. 998, 1983.

Kenneth P. Jackson (M'84) was born in Boulder, CO, in 1957. He began his undergraduate work at the University of California at Los Angeles and later transferred to the University of California at Berkeley where he received the bachelors degree in physics. In 1980, he received the masters degree in electrical engineering from Stanford University. Currently, he is at Stanford working on a Ph.D. in the fiber-optics group under the direction of H. J. Shaw. The emphasis of his work has been the application of optical-fiber technology to high-speed signal processing.

He has also participated in summer hire programs throughout his undergraduate studies. His work experiences have included the construction of lasers, analyses of semiconductor processing evaluation systems, and the development of fiber-optic local area networks.

Mr. Jackson is a member of the OSA.

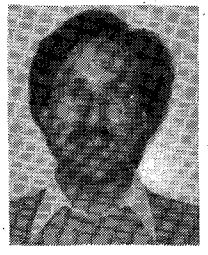

Steven A. Newton (S'81–M'83) was born in Teaneck, NJ, in 1954. He received the B.S. (physics) degree, summa cum laude, from the University of Massachusetts, Amherst, MA, in 1976. He received the M.S. and Ph.D degrees in applied physics from Stanford University, Palo Alto, CA, in 1978 and 1984, respectively.

His work as a Research Assistant at Stanford's Ginzton Laboratory involved fiber-optic rotation sensors, single-mode fiber components, and fiber-optic signal-processing devices. From 1978 through 1982, he was a part-time Member of the Technical Staff at Hewlett-Packard Laboratories, Palo Alto, CA, where he was engaged in research involving optical design, metal vapor lasers, and optical data storage. Since 1983, he has been a full-time Member of the Technical Staff at Hewlett-Packard Laboratories, where his research activities involve fiber optics, integrated optics, high-speed electrooptic devices, and systems. He is presently a Project Leader in the Wave Technology Department of HP's Physical Sciences Laboratory.

Dr. Newton is a member of OSA and SPIE.

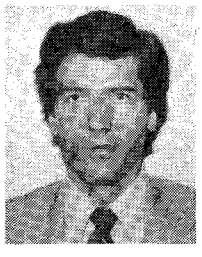

Behzad Moslehi (M'84) was born in Tehran, Iran, on August 11, 1956. He received the B.S. degree in electrical engineering from Tehran (Arya-Mehr) University of Technology, Tehran, Iran, the M.S. degree in electrical engineering, and the M.S. degree in applied physics from Stanford University, CA, in 1978, 1980, and 1984, respectively. He recently received the Ph.D. degree in electrical engineering also from Stanford University.

For his M.S.E.E. studies, he was with the Information Systems Laboratory of the Electrical Engineering Department, Stanford. For his Ph.D. studies, he has been working as a Research Assistant on fiber-optic signal processing at the Edward L. Ginzton Laboratory of Stanford since 1980. In this period, his research has focused on single-mode fibers. His Ph.D. dissertation topic is on fiber-optic lattice signal processing. He was employed by Xerox Corporation for one year in 1981, where he performed research on a new method of estimating the bandwidth of multimode optical fibers using speckle patterns generated by the fiber modal interference.

He is a member of the Optical Society of America and Sigma Xi. His research interests lie in fiber optics, quantum electronics, image processing, optical communications, and signal processing.

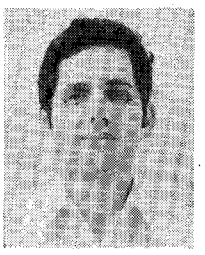

Moshe Tur was born in Tel-Aviv, Israel, in 1948. He received the bachelor degree in mathematics and physics from the Hebrew University, Jerusalem, Israel (1969), and the M.Sc. degree in applied physics from the Weizmann Institute of Science, Rehovot, Israel (1971), where he investigated electromagnetic wave propagation in distorted cholesteric liquid crystals. After spending five years with the Israeli Defense Forces, he attended the School of Engineering of Tel-Aviv University, Tel-Aviv, Israel, and received the Ph.D. degree in 1981. His research there involved analytical, numerical, and experimental investigations of wave propagation through random media as well as fiber-optic communication systems.

He spent the last two years at the Information Systems Laboratory and the Edward L. Ginzton Laboratory of Stanford University, Stanford, CA (a Postdoctoral Fellow in 1982 and a Research Associate in 1983). At the Information System Lab., he studied speckle phenomena, various theories of wave propagation through random media, and asymptotic solutions of the fourth moment equation. At the Ginzton Lab., he participated in the development of new architectures for single-mode fiber-optic signal processing and investigated the effects of laser phase noise on such processors.

He is presently a Senior Lecturer in the Interdisciplinary Department of the School of Engineering at Tel-Aviv University, Tel-Aviv, Israel. His current interests include fiber-optic devices and systems, as well as theoretical and experimental research on the effects of the turbulent atmosphere on various electrooptic systems.

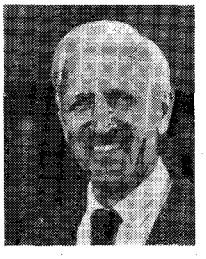

C. Chapin Cutler (A'40–SM'53–F'55–LF'80) received a B.S. degree in general science from Worcester Polytechnic Institute, Worcester, MA, in 1937, and took graduate courses at Stevens Institute of Technology, Hoboken, NJ.

Except for two short academic sabatticals, he was engaged in research at Bell Laboratories, Inc., Deal, Murray Hill, and Holmdel, NJ, from 1937 until 1979. His research included contributions to short-wave radio technology for over-seas communication, microwave radar antennas, microwave amplifiers, satellite communication technology, digital signal coding, and PICTUREPHONE®. He has been granted over 70 patents, including fundamental patents on Differential PCM, and propagation on corrugated wave guiding structures. He has held positions of Assistant Director of Radio and Electronics Research, Director of Electronic Systems Research, and Director of Electronic and Computer Systems Research. In 1979, he retired from Bell Laboratories to become Professor of Applied Physics at Stanford University, where he is engaged in research on microwave acoustics and applications of coherent optics. He was Sherman Fairchild Distinguished Scholar at California Institute of Technology in 1982–1983.

Mr. Cutler is a member of Sigma Xi and served as editor of *IEEE Spectrum* (1966–1967). He was awarded an honorary Doctor of Engineering degree from Worcester Polytechnic Institute (1975), was elected to the National Academy of Engineering (1970), and the National Academy of Sciences (1976). He received the Edison medal of the IEEE in 1981, the Robert H. Goddard Distinguished Alumni Award from Worcester Polytechnic Institute in 1982, and an IEEE Centennial medal in 1984.

Joseph W. Goodman (S'58–M'63 – SM'72 – F'74) received the A.B. degree in engineering and applied physics from Harvard University in 1958, and the M.S. and Ph.D. degrees in electrical engineering from Stanford University in 1960 and 1963, respectively.

He joined the research staff at Stanford in 1963 as a Research Associate. In 1967, he was appointed Assistant Professor, and since 1972 he has been a Professor of Electrical Engineering. During the academic year 1973–1974, he was a Visiting Professor at the Institut d'Optique, Orsay, France.

He chaired an IEEE *ad hoc* Committee on Optical and Electro-Optical Systems in 1969, and served on the Editorial Board of the *Proceedings of*

the IEEE for the years 1979 and 1980. He has also been a member of the Fellows Committee of the Santa Clara Valley Section of the IEEE for several years.

For the Optical Society of America (OSA), he was elected a Director-at-Large for the years 1972–1974; he also served on the Board of Directors *ex-officio* through 1983 in his capacity as Editor of the *Journal of the Optical Society of America*, a position he held for the years 1978–1983.

For the International Optical Engineering Society (SPIE), he was elected to the Board of Governors for the years 1980–1982, and has served as a member and Chairman of the Awards Committee, as a member of the Nominating Committee, and as a member of the Publications Committee and the Technical Council.

Dr. Goodman is a Fellow of the OSA and the SPIE. In 1971, he was chosen recipient of the F. E. Terman award of the American Association for Engineering Education. He received the 1983 Max Born award of the Optical Society of America, for his contributions to physical optics, and in particular to holography, synthetic aperture optics, image processing, and speckle theory. He is the author of more than 100 technical publications, including the textbooks *Introduction to Fourier Optics* (1968) and *Statistical Optics* (1984). He is listed in *Who's Who in the West*, *Who's Who in America*, and *International Who's Who in Engineering*.

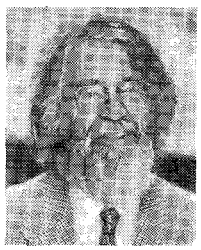

H. J. Shaw (M'55–F'73) was born in Seattle, WA, and received the B.A. degree from the University of Washington and the Ph.D. degree from Stanford University. He is presently a Professor (Research) at Stanford University. He has been engaged in the past in research on microwave antennas and high-power microwave tubes, microwave ferrite devices involving resonance and spin waves, microwave acoustic devices including thin-film transducers, bulk-wave delay lines and acoustooptic signal processors, and surface acoustic-wave devices including transducers, delay lines, amplifiers, convolvers, matched filters, and optical scanners. His present activities involve research on sensing and signal processing using optical fibers, on real-time acoustic imaging systems, and on piezoelectric polymer devices.

He has been a consultant to a large number of electronic firms. During 1968–1969, he was Liaison Scientist for the U.S. Office of Naval Research in London. He is a member of Tau Beta Pi and recipient of the 1976 Morris N. Liebmann Memorial Award of the IEEE "for contributions to the development of acoustic surface wave devices," and the 1981 Achievement Award of the IEEE group on Sonics and Ultrasonics "for many contributions, through research and education, to ultrasonics technology."

Graphic Design of Matching and Interstage Lossy Networks for Microwave Transistor Amplifier

JUAN CARLOS VILLAR AND FÉLIX PÉREZ

Abstract—**A graphical design method for lossless and lossy gain-compensating networks is presented, and the advantages of the use of this technique in the construction of microwave transistor amplifiers are discussed. The method is based on the use of a set of constant $|S_{ji}|$ circles plotted on the Smith Chart, and is easily automated on a personal computer. Two applications are presented: a two-stage amplifier with 20 dB in the 100–1100-MHz band and an ultra-broad-band lossy matched amplifier stage with 4 dB in the dc–16-GHz band.**

I. Introduction

IN ORDER TO DESIGN wide-band microwave amplifiers, it is necessary to compensate for transistor gain roll-off with frequency. Usually this compensation is achieved by lossless coupling networks which reflect unwanted available power for low frequencies. Several analytical design techniques for lossless equalizers have been reported [1], [2], like the well-known constant gain circles graphic method [3]. However, these techniques are not satisfactory in many cases, and lossy equalizers must be employed to obtain a flat gain response, especially in the design of ultra-wide-band amplifiers.

Several design methods for lossy equalizers have been reported. However, particular networks have been proposed by these authors, yet their methods cannot be applied to all configurations [4], [5]. This paper presents a new graphic design method with a wider field of application, which allows us to calculate matching and interstage lossless and lossy networks with any configuration, and is an excellent first step in the design of wide-band amplifier modules. The technique is similar to the constant gain circles method, and is based on the use of a set of curves of constant $|S_{ji}|$, plotted on the Smith Chart, that leads in a simple way to the structure of the networks in order to obtain gain equalization and matching in the transistor ports. Additional advantages of this procedure are the

Manuscript received June 6, 1984; revised October 9, 1984.

The authors are with the Departamento de Microondas, E.T.S.I. Telecomunicación, Universidad Politécnica de Madrid, Cindad Univerzsitaria, Madrid-3, Spain.

0018-9480/85/0300-0210$01.00 ©1985 IEEE